PROTOTYPE CARBON FIBRE PROPELLER DEDICATED FOR HYBRID POWER UNMANNED AERIAL VEHICLES WITH MTOW UP TO 300KG

Małgorzata Wojtas, malgorzata.wojtas@ilot.lukasiewicz.gov.pl Institute of Aviation (Poland)

Przemysław Wyszkowski, przemysław.wyszkowski@ilot.lukasiewicz.gov.pl Institute of Aviation (Poland)

Paweł Kmita, paweł.kmita@ilot.lukasiewicz.gov.pl Institute of Aviation (Poland)

Maciej Osiewicz, maciej.osiewicz@ilot.lukasiewicz.gov.pl Institute of Aviation (Poland)

Abstract

The article presents concepts of a technology demonstrator of a hybrid – electric propulsion system (HEPS) for new generation of VTOL Unmanned Aerial Vehicles with a take-off weight of up to 300 kg. The motivation to undertake such works is the increasing use of heavy drones in relation to the currently produced electric drones with low payload. The main assumption of the demonstrator project was to use commercially available components. In preliminary phase of the project, a market analysis were conducted in terms of available: propellers/rotors, drive units, generators, electric motors, and energy management systems. First version of the system was designed as four-rotor system demonstrator. This article presents the design approach and test results in general. In the following chapters, authors introduce a six - rotor development version of the demonstrator. However the main focus is put on the propeller designed for the development version of the technology demonstrator. Assumptions of the new composite propeller design are shown. The paper briefly discusses aerodynamic calculations and obtained results, which were the basis for the propeller design and its manufacturing. Furthermore, the testing method of prototype propeller, test system for dynamic models and research results are presented. In conclusion authors presented encountered problems during the design and tests and obtained tests results. Moreover, further development directions are discussed.

1. GENERAL INTRODUCTION

The area of Unmanned Aerial Vehicles (UAVs) has seen rapidly growth over the last years. The one of the main reason for the increase in use and development of unmanned aircraft is their ability to effectively carry out a wide range of applications with low cost and without putting human resources at risk. Currently, the main emphasis is on the development of vertical take-off and landing drones. The development of electric drives, more efficient power sources and the increasing possibilities of microprocessors allowed for the creation of numerous structures, usually of small size and weight around 50 kg. Such objects are controlled by changing the rotational speed of individual rotors, which changes their thrust and resistance torque. That allows for simplification of the dynamics and aerodynamic control system with such a structure compared to classic rotorcraft systems. The issues of flight of this UAVs are also very simplistic, the main focus is put on the control system. In the literature, it is usually assumed that the propeller thrust is directly proportional to the square of their rotational speed and that the propeller force acts exactly along the axis of the powerplant. Nonetheless, these solutions are being transferred to drones with higher take-off weights above 200 kg. This is forced by the development of urban flight mobility - passenger drones (air taxis) and cargo drones. Contrary to unmanned air taxis, which are in the demonstration phase for now, cargo drones are a proven technology. They can deliver online orders, drop vital medicines to places where normal deliveries are difficult or impossible, or zip around warehouses delivering parts at the precise moment they're needed [3].

The article presents the work carried out on the technology demonstrator of a hybrid powered VTOL Unmanned Aerial Vehicles with a take-off weight of up to 300 kg. The motivation to undertake such works is the increasing use of heavy drones in relation to the currently produced electric drones with low payload. Two concepts are presented, at first, technology demonstrator with four rotors, further six-rotor concept is discussed.

The paper presents among others: a summary of components used in the demonstrators design and

manufacturing, results from bench tests and analyzes for four-rotor technology demonstrator.
The main focus is on the selection of propellers. Preliminary analyzes and bench tests for various propellers (commercially available) and their configurations were prepared.
Furthermore, propeller design concepts for a 6 - rotor (or n-rotor) unit is shown. The results of analyzes and the aerodynamic design are briefly presented. Then the paper discusses manufacturing method of propeller blades and hub. The main part of the presented work in chapter 3 refers to the propeller for multi-rotor VTOL systems, presents and discusses a number of tests carried out on the test stand and on the system dynamics model compared to aerodynamic results.

2. TECHNOLOGY DEMONSTRATOR

The technology demonstrator of a multi-rotor aircraft hybrid power system is presented and discussed below. This work was undertaken due to the fact that vertical take-off drones without additional launch systems (like launchers, rocket motors, etc.) rely solely on rotor systems. In the currently used drones with a take-off weight of up to 300 kg, a classic main rotor system with a tail rotor is used, in rare cases the design is based on coaxial rotor systems.
In preliminary phase of the project, market analysis was conducted in terms of availability: propellers, drive units, generators, electric motors, and energy management systems.

2.1. Commercial propellers – overview

One of the essential tasks of hybrid electric propulsion system demonstrator design was to review and analyze propellers and rotors already available on the market, that meet the project assumptions. The basic criterions for the selection of propellers were required thrust to consumed power ratio and their availability in the right and left-hand rotation variant The propellers for two variants: the 8 + n rotor system and 4 - 6 rotor system were considered.
Selection of propellers is discussed below, presented results were obtained from the tests performed on test bench. The outcomes of the performed tests are presented in the following subsections.

2.1.1. 8 + n rotor system

Multirotor system propellers from Multistar, Dynam and Quanum in several variants were tested first.
Selected propellers were tested in system with Turnigy RotoMax 150cc electric motor. The propeller installed on the test stand is presented below in Figure 1.

Fig. 1. The propeller (*R380 30x5.5)* with Turnigy RotoMax 150cc electric motor

The graphs below show the characteristics of the tested propellers in a system with an electric motor (Figure 2 and 3).

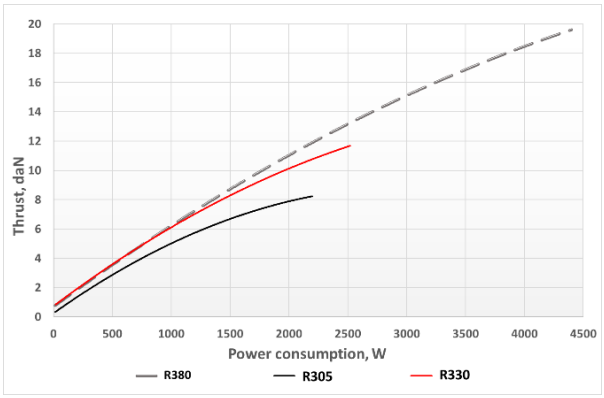

Fig. 2. Propeller R380, R305 and R330 characteristic with Turnigy RotoMax 150cc electric motor

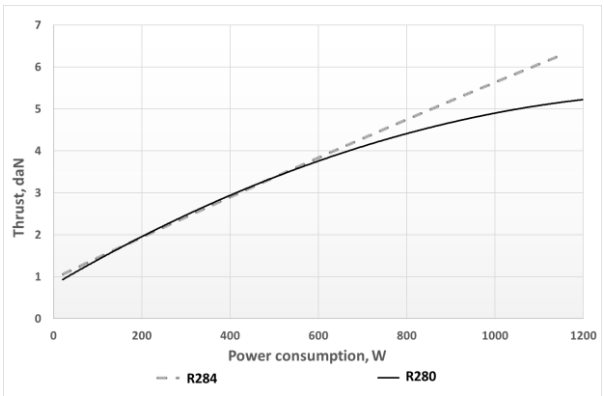

Fig. 3. Propeller R284 and R280 characteristic with Turnigy RotoMax 150cc electric motor

2.1.2. 4 - 6 rotor system

Under second multirotor system, after analyzing the market of commercially available left and right-hand rotation propellers meeting the project requirements, Peszke and Aerobat propellers were selected for tests. Propellers produced by these manufacturers met the conditions of having right and left-hand rotation variants and the size

ensuring appropriate power consumption for thrust production enough for a 4-6 rotor system.
Peszke propellers were selected in 2 and 3 blade variants. Two-blade propeller in two versions, right and left rotating. These propellers also have the possibility of changing the angle of attack of blades. The Emrax 188 electric motor was used to test the above-mentioned propellers. Propellers were tested on similar stand as presented in the previous section.
Families of characteristics obtained for Peszke *AS 1250/700-A-2B* and *AS 1250/700-A-3B* propellers (in the anti-clockwise version) are presented below. The analyzes are presented for two-blade and three-blade propellers at different angles of attack. Figures 4 and 5 show the relationship between the thrust and the power consumed by the propeller at variable rotational speed. Figure 6 shows the characteristics of Peszke 2-blade propellers. The characteristics were made for a constant rotational speed with a variable blade angle of attack. They represent propeller thrust versus power consumption.
The analyzes were also carried out for the Aerobat 54 inch wooden propeller with a fixed angle of attack. Below (Figure 7) are the propeller characteristics for variable rotational speeds compared to the Peszke propeller (2-blade propeller with an angle of attack of 12 degrees).

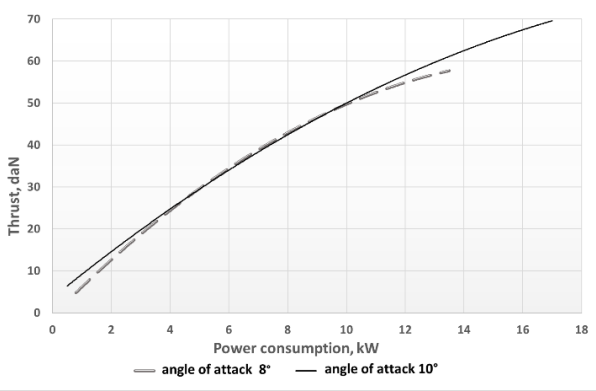

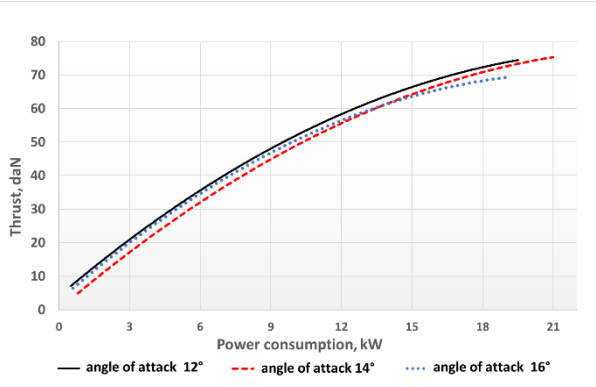

Fig. 4. Peszke 2 - blade propeller characteristic with electric motor EMRAX 188 for different angles of attack under variable rotationa speed

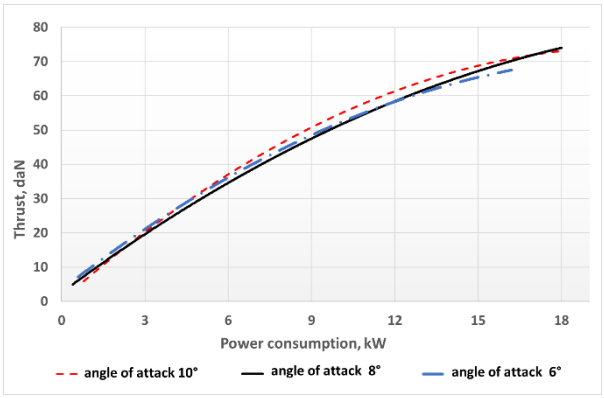

Fig. 5. Peszke 3 - blade propeller characteristic with electric motor EMRAX 188 for variable rotational speeds

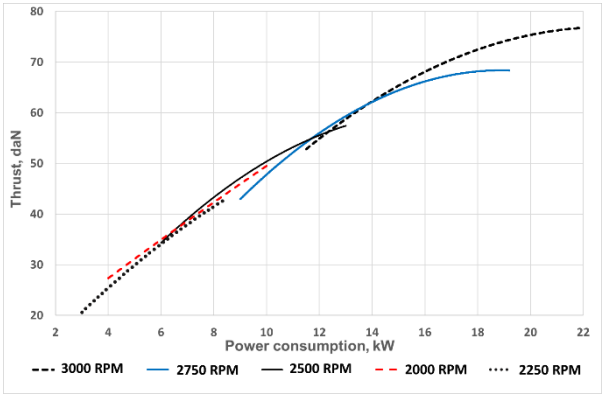

Fig. 6. Peszke 2 - blade propeller characteristic with electric motor EMRAX 188 for variable angle of attack

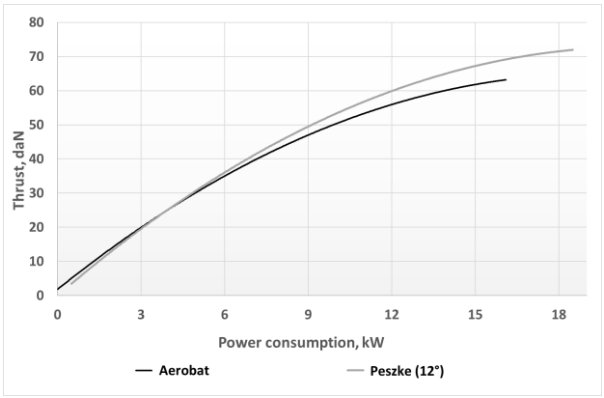

Fig. 7. Aerobat propeler characteristic with electric motor EMRAX 188 and Peszke 2 - blade propeller characteristic (12º) with EMRAX 188 electric motor for variable angle rotational speed

Table below (Table 1) summarizes the results of tests and analysis of the discussed propellers from section 2.1.1 and 2.1.2. The table includes, inter alia, the power density, voltage, peak thrust and peak power, for each tested electric motor – propeller pair.
For the demonstrator design, Aerobat propellers were used, mainly due to fairly good parameters obtained in preliminary tests, and to their quick availability in high amount both in clockwise and anti - clockwise rotational version.

Tab. 1. Preliminary selection of propellers – test results

Name	Peak Power kW	RPM	Peak Thrust kg	Power density kg/kW	Voltage [V]	Motor	VTOL Config
R380 30x5.5	4.6	5400	20	4.3	44.4	Turnigy RotoMax 150cc	8 + n rotors
R330 26x5.5	1.9	3800	10	5.3	44.4	Turnigy RotoMax 150cc	8 + n rotors
R305 24x5.5	1.6	3800	6	3.8	44.4	Turnigy RotoMax 150cc	8 + n rotors
R284	1,0	4000	6	6.0	44.4	Turnigy RotoMax 150cc	8 + n rotors
R280 22x5.5	1.2	4000	5	4.2	44.4	Turnigy RotoMax 150cc	8 + n rotors
AS 1250/700-A-3B 	18	2800	75	4.17	355.2	Emrax 188	4 – 6 rotors
AS 1250/700-A-2B 	18	3000	76	4.22	355.2	Emrax 188	4 – 6 rotors
Aerobat (1180mm) 	12	3000	50	4.17	355.2	Emrax 188	4 – 6 rotors

2.2. 4 - rotor HEPS demonstrator

The project began with designing and building a technology demonstrator with 4 rotors (propellers). The aim was to construct a test platform from the elements available on the market. In the first stages of demonstrator development, all components had been assembled according to the Table 2 presents the list of elements.

Tab. 2. Four – rotor demonstrator elements

Power unit	1		Yamaha YZF-R1 engine	133,9 kW/12.5k RPM /92 kg
Executive unit	4		EMRAX 188	32 kW/ 4.5k RPM / 6.8 kg
Drivers	4		Bamocar D3	8,5 kg/liquid cooling
Generator	1		EMRAX 268	110 kW/ 4.5k RPM / 20.3 kg
Propeller	4		Aerobat	1180 mm/ wooden /1.14kg

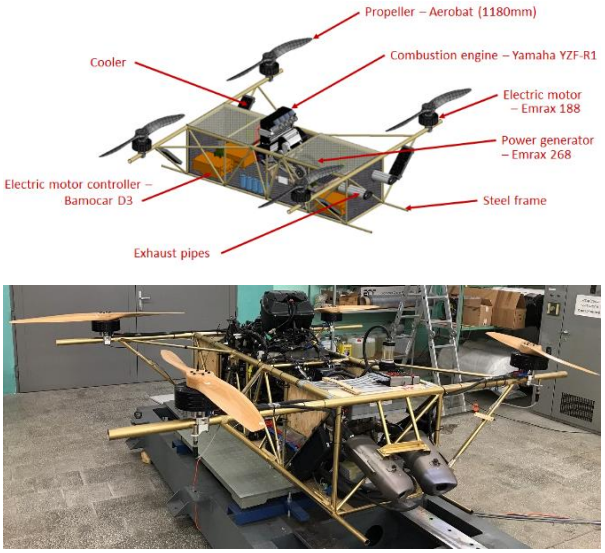

Fig. 8. Technology demonstrator of hybrid system

The power source is the YAMAHA R1 internal combustion engine directly connected by means of mounting elements to the EMRAX 268 electric motor, which in this case works in generator mode. The torque is transmitted via chain gear. The combustion engine has a built-in gear that is engaged by a friction clutch. The torque from engine to the generator is transmitted via chain gear. The generator is connected to a diode rectifier which, through a system of super-capacitors, is connected to four Bamocar D3 drivers that control the operation of the executive motors – Emrax 188.

2.2.1. Tests resuls

Tests were performed in several stages. The results of the test with the maximum set parameters for the presented system are shown below (Figure 9). After initial tests for low rotational speeds of propellers were completed, tests with the target system speed of 2500 RPM were started. Entire system thrust is 210 daN, the power demand of electric motors with propellers is about 30 kW, the power density of the executive motor is 7 kg/kW.

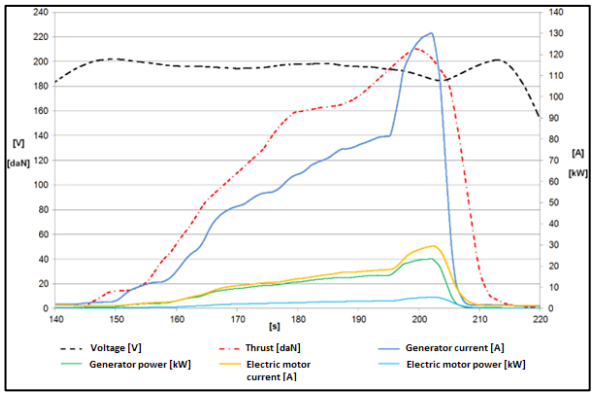

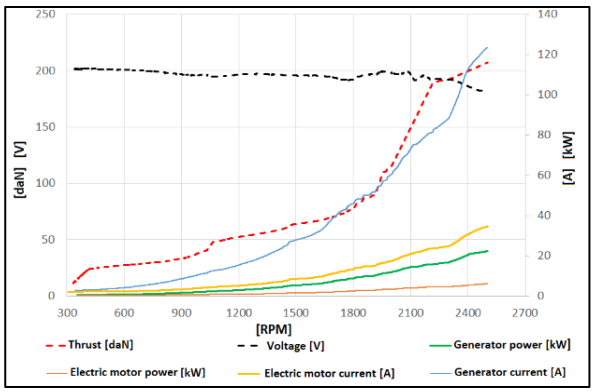

Fig. 9. Characteristics of the demonstrator parameters depending on the rotational speed (electric motors – propellers)

Despite the satisfactory results of the first tests, change of the drive unit (internal combustion engine) was necessary. The reason was that the engine overheated during tests.

2.3. 6 - rotor demonstrator concept

After collecting all the required data from the four-rotor demonstrator tests, preliminary analysis of the system dynamics and the control possibility of the VTOL platform as well as assumptions for the next version of the demonstrator have been prepared. The main assumptions for the target system six - impeller unmanned vehicle, shown in figure 10, are:

- implementation of bigger and more efficient rotors in order to provide more thrust,
- consideration of more powerful electric motors to provide sufficient power and torque to the propellers,
- redesigning the frame and mounting of the power generator to be more lightweight,
- use of CFRP composites for further weight reduction.

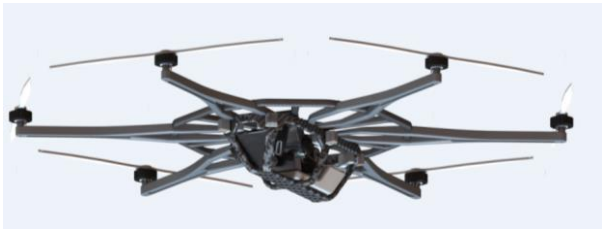

Fig. 10. Visualization of multi-rotor unmanned vehicle

In the next version of the demonstrator, some general changes and new solutions were proposed. The Table 3 presents the list of elements set to use in new HEPS demonstrator.

Tab. 3. Six - propeller demonstrator elements

Power unit	1		BMW S1000RR	146 kW/ 13.5k RPM / 75 kg
Executive unit	6		EMRAX 208	41 kW/ 4.5k RPM / 9.1 kg
Drivers	6		Bamocar D3 in carbon composite housings	7.5 kg/ air cooling
Generator	1		EMRAX 268	110 kW/ 4.5k RPM / 20.3 kg
Propeller	4		Ł-ILOT design	1998 mm / prepreg carbon composite, 3.6 kg (with test hub)

3. PROPELLERS

One of the main tasks performed for this unit was the design of a new generation composite propeller. Design assumptions specifying the requirements to be met by the rotor have been determined on the basis of the target mass of the multirotor and its operating conditions. Table no1 summarizes these requirements.

Tab. 4. Design assumptions

MTOW	350 kg
Ceiling	<500 m
Rotors number	6
Lifting force per rotor	572.5 N
Max power per rotor	15 kW
Max motor torque	70 Nm
Max rotor diameter	2 m

One of the basic rotor design assumptions is fixed geometry, without the possibility of changing collective pitch as in classic rotorcrafts. The rotorcraft is controlled by changing the rotation of individual motors, while the forward flight - by tilting the entire unmanned aerial vehicle. Due to the planned cruising speeds in excess of 100 km/h, there is a significant compromise between the geometry of the optimal rotor for hovering and forward flight. Based on the market analysis and design assumptions, the first goal of the design work was determined - hovering at sea level should be possible with a power of not more than 8kW per rotor. The above target therefore assumes an efficiency of 7.3 g/W. This value is used as a benchmark.

Taking into account the design information briefly given above, an in-depth aerodynamic analysis was performed and the propeller profile and geometry were proposed. Then the design and prototype of propeller was manufactured by analyzing the commercial solutions and the guidelines contained in the CS-P aviation regulations.

3.1. Aerodynamic design

This chapter generally discusses the course of calculations and the aerodynamic design for the new propeller. A detailed description of the project is included in the literature [4].

The designed rotor, apart from providing the required thrust at the lowest power, must meet a number of requirements. They result from the manufacturing technology, structural strength and assumed operating conditions. One of the constraints adopted at the beginning of the design was the pre-selected manufacturing technology using prepreg composites which places limits on the thickness of the trailing edge. In calculations, a constant thickness of the trailing edge for the entire blade was assumed to be 1 mm. Another significant technological requirement by blade design is the leading edge radius. The minimum value for the radius is set to 0.5 mm, this limitation is of particular importance near the tip of the blade. Not only are thinner profiles used there, but the chords are also smaller.

The analyzes were performed for hover and forward flight of the VTOL vehicle.

3.1.1. Calculation methods

Several calculation methods were used to design the propeller. Initially, the analyzes were carried out by the low-fidelity Blade Element Momentum Theory model, the parameters defining the optimum blade geometry were found using extensive evolutionary search [4, 7, 8, 12]. The results of the search process using BEM and the evolutionary algorithm provide contour parameters on the basis of which a three-dimensional rotor model should be built. At the current stage of research, it was decided to arrange the profiles on individual radii assuming a fixed point of the quarter chord (Figure 11).

The next step was to optimize the propeller blade airfoil. The RANS method was used. In the first step of the aerodynamic analyzes, the results obtained with the BEM were compared. A stationary aerodynamic model of the rotor in the hover was built. The results of the RANS

calculations for the hover confirmed the validity of the BEM design approach. A satisfactory agreement was obtained between the lift force and torque for given rotational speeds between both methods. The differences did not exceed 10% for the operating conditions of the rotor.

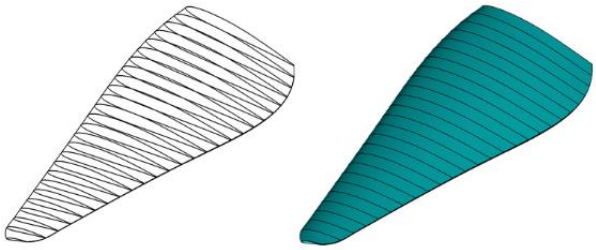

Fig. 10. Optimum blade geometry for fixed profile - base geometry [4]

Then, calculations for the forward flight (level flight) of the multirotor were prepared. Such flight is a critical case. This is caused by the asymmetric load on the blade, which results in a significant change in the pressure distribution on its surface. In order to perform the calculations, the more advanced method was used. The flow in this case requires a non-stationary calculation (URANS) for the whole rotor model, i.e. without symmetry/ periodicity.

3.1.2. Results

Below is a visualization of the propellers geometry for the performed calculations, are shown in figure below (Figure 12).

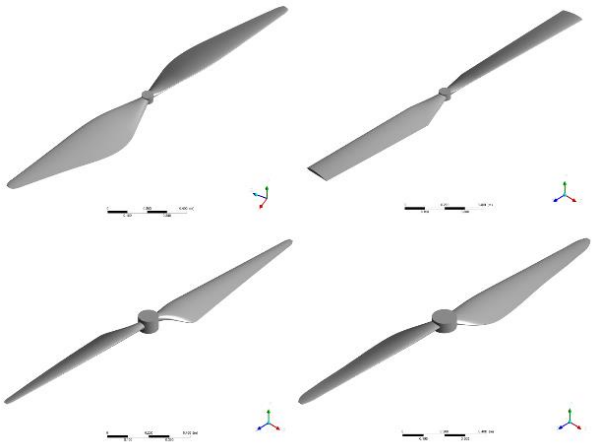

Fig. 11. Four propellers obtained in the design process: propeller with a constant profile (upper left), with a constant profile, chord and linear twist (upper right), with a linearly variable chord (lower left), and with any parameters (lower right) [4].

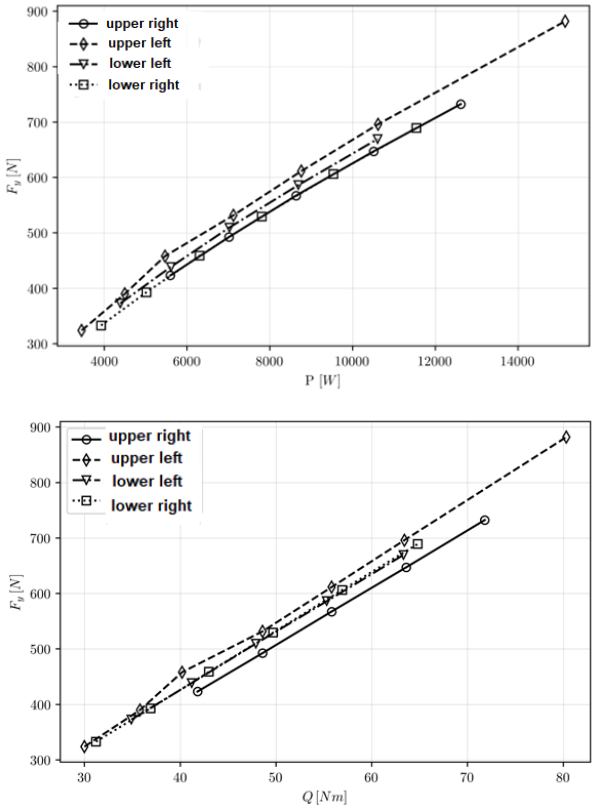

Fig. 12. Propellers obtained in the design process - characteristics: propeller with a constant profile (upper left), with a constant profile, chord and linear twist (upper right), with a linearly variable chord (lower left), and with any parameters (lower right) [4].

Figure 13 shows the characteristics of propellers obtained in the design process. The most efficient is the rotor with a fixed profile, which does not meet the structural constraints. The use of structural constraints slightly worsens the characteristics of the rotor. The weakest, as expected, is the rotor designed with the greatest limitations - straight. Not only does it fail to satisfy the structural constraints, but also requires a higher torque.
A summary of the lifting force and torque for the final propeller is presented in Table below (Table 5).

Tab. 5. Summary of hover results for final propeler design

Rotational speed, RPM	Lift force N	Torque Nm
1300	445.4	40.4
1400	519.4	47.1
1500	596.2	54.2
1700	767.6	70.2
1800	859.0	78.1

3.2. Design and manufacturing

Initially, an overview of technological solutions available on the market was prepared. Most manufacturers use epoxy-based composites reinforced with carbon and glass fibers. Originally, "wet" supersaturation was used, but nowadays, resin infusions / injection into closed molds are already used on a larger scale, in which there is already reinforcement. The second widely used technology are prepregs (reinforcement saturated with a strictly defined amount of uncured saturating mixture). Several propeller blade and hubs design are shown below (Figure 14 and 15).

Fig. 13 Examples of propeller balde design and manufacturing [14, 15, 16].

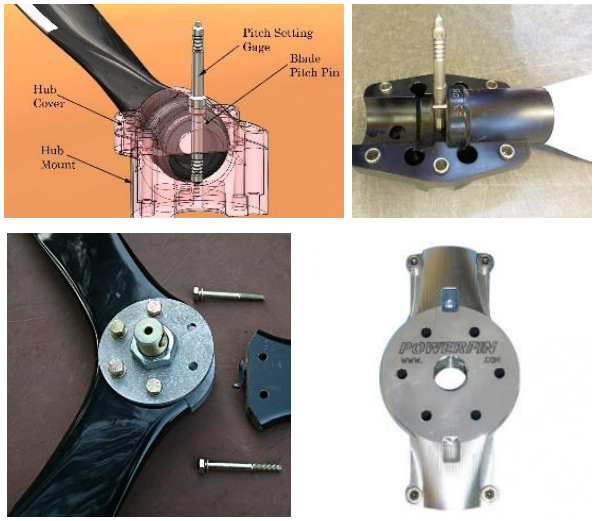

Fig. 14 Examples of propeller mounts / hubs [14, 15, 16]

By far the most common solution for mounting the blade in the hub is to make the tip of the blade in an axisymmetric shape. This allows for any setting of the wedge angle i.e. the propeller pitch, of the blade. The possibility of the radial protrusion of the blade is eliminated by a positive fit. Some manufacturers also use the reverse configuration. The possibility of rotating the blade in the hub (pitch change is eliminated by pinching the blades between the hub halves.

3.2.1. Multirotor propeller design

Based on the experience of the Composite Technologies Center in design and manufacturing rotors blades in prepreg composites technology, presented in literature [5, 9], a propeller design and manufacturing technology was developed.
At the first stage of the project, the requirements were defined based on the aviation regulations of CS P. The following requirements are defined [1]:

- CS-P 240 - static strength, the minimum strength margin factor, calculated in relation to the permissible loads, must be at least 2.0
- CS-P 530 - Vibration and aeroelasticity, the structure must be free from resonance in the range from 0 - 2.0 times nominal propeller revolutions.

Further in subsequent phases of the project, based on the aviation requirements above and aerodynamics calculation, the general design and strength calculations were prepared. After that, the selection of composite materials (m.in. prepregs) and the development of the target propeller manufacturing technology were started.
Finally, the multi-rotor propeller was designed as a combination of two composite blades connected with aluminum hub. The hub was design in such way that it allows to set propeller blades angle of attack. Visualization of the propeller with the hub is presented below (Figure 16).

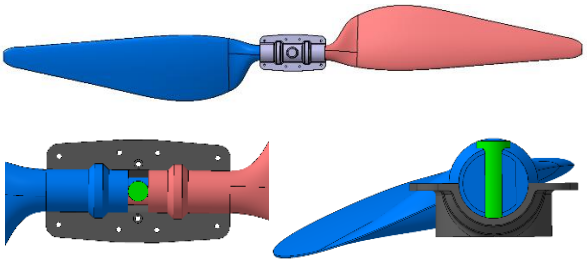

Fig. 15. General design of a propeller with a hub – visualization

The blade structure consists of a spar with an upper and lower sheathing glued to it. The space between the sheathings is filled with a special foam. The covers and the spar are made with carbon fabrics and tapes. The prepared propeller is presented below (in Figure 17 - without and after varnishing).

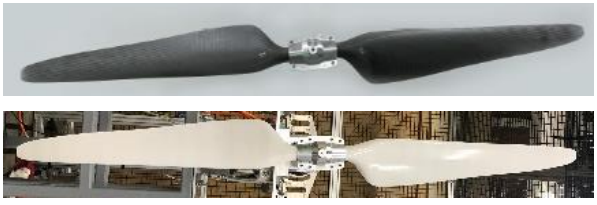

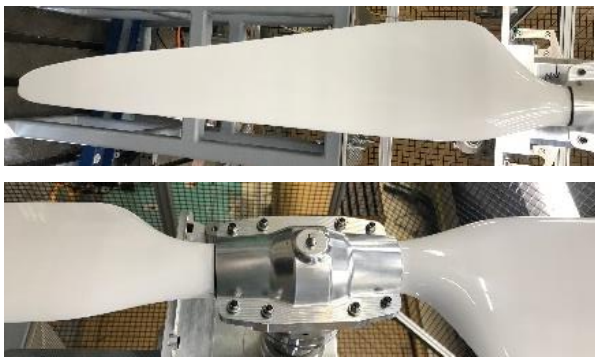

Fig. 16. Prototype propeller for unnmaned VTOL systems

4. PROPELLER TESTS

4.1. Measurement method

Experience shows that bench tests put significant impact on the prototyping process. Research on incl. helicopter and gyroplane rotors at Whirl Tower stands, allows to obtained lot of information about the tested object and confirm the design assumptions. More information is available in the literature [2, 6, 10,11,12].

4.1.1. Test stand

The measuring stand for testing the parameters of propellers and rotors in the hover was made as one of the stages of the Hybrid Drive Dynamometer project. Discussed test stand (Fig. 18) allows for testing propeller and rotors with diameter up to 2.4 m, which can be used, inter alia, in VTOL type multi-rotor drone systems. This solution allows for testing propellers in system with electric motors. To certain extent, it is possible to change electric motors, power supply systems and measuring sensors, to increase the measuring range.
The figure below shows the thrust test stand and its simplified design and components, where: 1 – propeller mounting hub, 2 – bearing assembly, 3 – torque meter carriage, 4 – torque sensor, 5 – electric motor, 6 – electric motor carriage, 7 – swivel joint, 8 – thrust sensor, 9 – mounting frame.

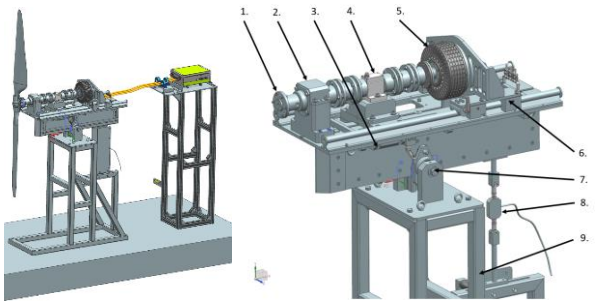

Fig. 17. Propeller thrust test stand - visualisation

The principle of operation of the stand is based on the method of balancing the moments. This type of method allows to maximize the efficiency of the entire team and to avoid the need to use correction factors.

Fig. 18. Propeller thrust test stand

4.2. Dynamic model

4.2.1. Test stand electric diagram

Figure 20 shows a general electrical diagram of the stand. supply.

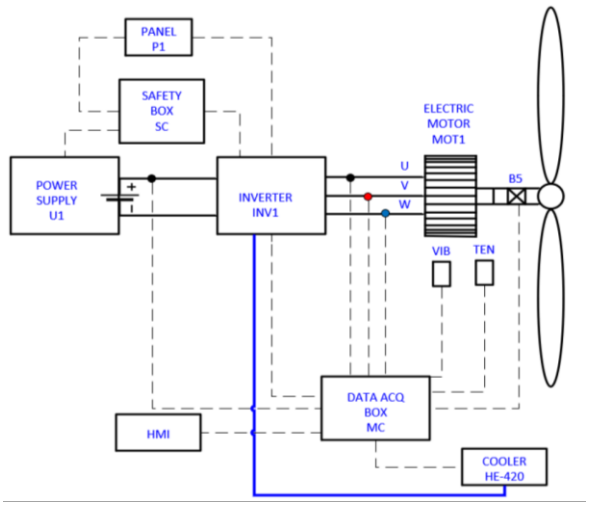

Fig. 20. Propeller thrust test stand – electrical diagram

The tested propeller is driven by an electric motor (in this case EMRAX 188) - MOT-1, which is connected to the tested object (rotor/propeller) by means of couplings and a torque sensor - B5. The electric motor is controlled by the BAMOCAR D3 - INV1 inverter, which is powered by a bidirectional voltage source 500V/120A/18kW - U1. The inverter is liquid-cooled via the water-air heat exchanger - HE-420. All measurements are transferred to the HMI via NI's cRIO-based data acquisition system in a box - MC. The application installed on a PC is an interface for the exchange of information between the operator and the system and enables the preview of the measured values. The inverter is controlled by the control panel (P1) next to the operator. The safety system is handled by the safety box (SC) in which there is a safety relay that

disconnects the PWM output signal of the inverter power and the DC.

4.2.2. Test stand dynamics model

The general model of the dynamics of the test stand for testing rotors and propellers, discussed in chapter 4.1.1, is presented below (Figure 21).

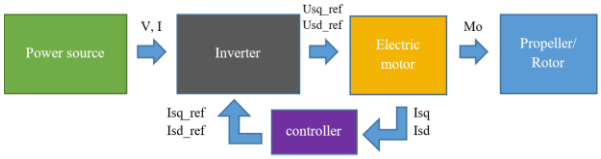

Fig. 19. Dynamic model - block diagram

In the dynamic model design all major components of the device (test stand) are taken into account. The following blocks from the diagram shown are discussed below.

4.2.3. Electric motor mathematical model

Permanent magnet synchronous motors in some classifications are divided into PMSM sinusoidal electromotive force motors and trapezoidal electromotive force motors, also called brushless DC motors (BLDC) [13]. For applications where high dynamics, low electromagnetic torque pulsations and a large speed range are required, the PMSM type motor is the best choice. The basic dependencies and describing a permanent magnet synchronous motor (PMSM) are as follows:

$$u_d = R_s i_d + \frac{d\psi_d}{dt} - p\omega_m \psi_q \quad (1)$$

$$u_q = R_s i_q + \frac{d\psi_q}{dt} - p\omega_m \psi_d \quad (2)$$

The equations that bind the magnetic fluxes are:

$$\psi_d = L_{sd} i_d + \psi_f \quad (3)$$

$$\psi_q = L_{sq} i_q + \psi_f \quad (4)$$

Where: u_d, u_{do}, u_{dd}, u_q, u_{qo}, u_{qq}, i_d, i_q, L_s, R_s, ψ_f, p, are respectively the voltages and currents in the rectangular coordinate system dq, inductances, resistances, flux from permanent magnets and the number of pole pairs. The electromagnetic moment can be determined from an approximate, where: K_t is the structural constant:

$$M_e \cong \frac{3}{2} p\psi_f i_q \cong K_t i_q \quad (5)$$

The equation of motion is analogous to the equations for the previously described devices and can be written in the form:

$$\frac{\omega_m}{dt} = \frac{1}{J_z}(M_e - M_o) \quad (6)$$

Where: ω_m, J_z, M_o mean the angular velocity, equivalent moment of inertia of the engine and working devices, and the load moment, respectively. Based on the equations describing the synchronous device in a rotating rectangular coordinate system, a simulation scheme of the PMSM motor can be built.

4.2.4. Electric motor regulators

The basic regulation structure for a permanent magnet synchronous motor drive is shown in Figure 22. Two control paths of the stator current components can be distinguished in the *d* and *q* axes, respectively. For motors with permanent magnets placed on the rotor surface, the value of the current in the d axis is set to zero. The current value in the *q* axis will then determine the electromagnetic moment developed in the motor. The implementation of the field-oriented control method requires the measurement of the angular velocity of the rotor and the currents in two phases. The instantaneous values of the phase currents are first converted to a stationary rectangular frame of reference, and then, using the information on the angular position of the rotor γr, transformed to the rotating rectangular coordinate system xy (which will be alternatively also referred to as the dq system). The current regulators in the *d* and *q* axes usually have the structure of a PI regulator.

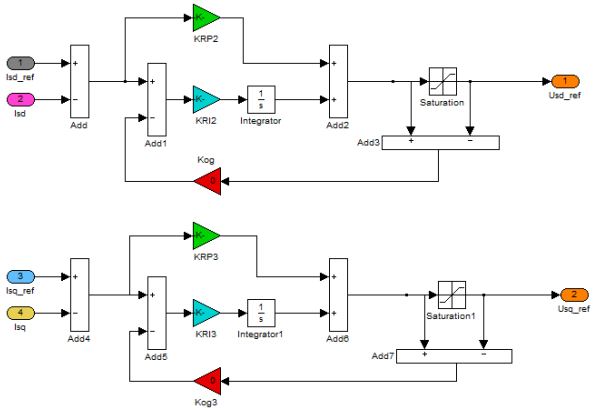

Fig. 20. Construction of regulators in the Matlab Simulink program

4.2.5. Propeller model

When modeling the test object, we must take into account the moments of inertia of the propeller, propeller hub and the shaft that transmits the engine torque to the propeller.

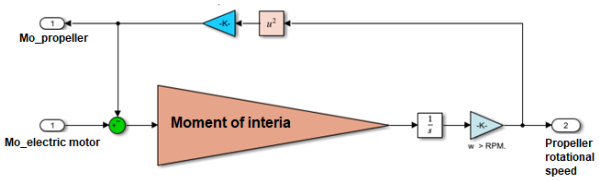

Fig. 21. Propeller model with moments of inertia

Above, in Figure 23, propeller model design in Matlab Simulink environment.

4.3. Bench tests resuls

The bench tests were carried out as follow: wooden Aerobat propeller, ILOT carbon composite propeller. The research results are presented below.
In the first graph (Figure 24) presented thrust as a function of the power consumption by propeller. The results of the experiment were compared with the results of the dynamic model.

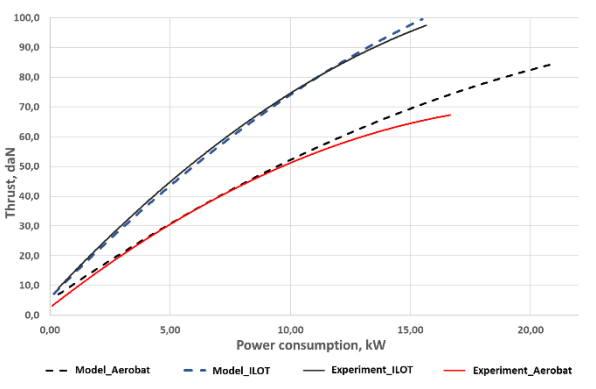

Fig. 22. Test bench and model results comparison for Aerobat proppeler and ILOT propeller

The following charts present the results for the composite propeller developed in Institute of Aviation. Graphs below show a comparison of the results from the aerodynamic analyzes, dynamic model tests with data obtained from the test bench experiment.
The charts show accordingly: thrust as a function of the propeller power consumption (Figure 25), thrust as a function of the propeller rotational speed (Figure 26), thrust as a function of torque on the shaft connecting the propeller and the electric motor (Figure 27). Analyzes were carried out for the variable rotational speed of the propeller.

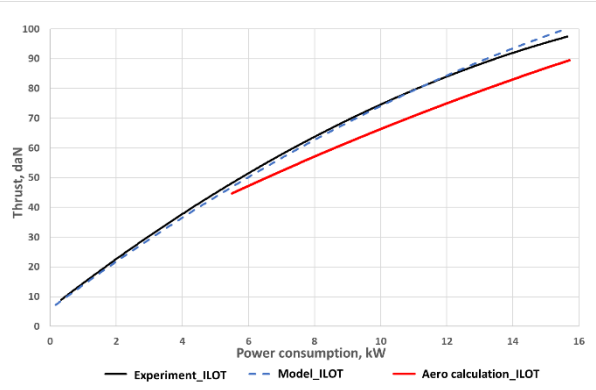

Fig. 23. Test bench aerodynamic analyzes and model and comparison for ILOT propeller - thrust as a function of the power consumption

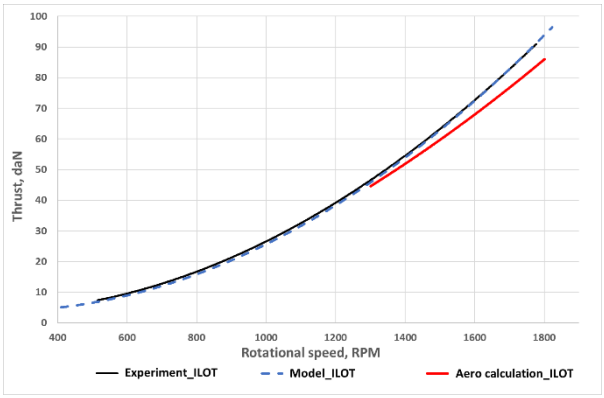

Fig. 24. Test bench aerodynamic analyzes and model and comparison for ILOT propeller - thrust as a function of the rotational speed

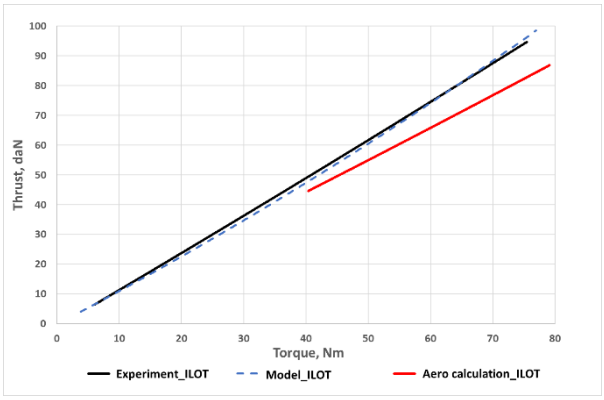

Fig. 25. Test bench aerodynamic analyzes and model and comparison for ILOT propeller - thrust as a function of torque

5. CONCLUSION

The works discussed in this study concern multi-rotor with hybrid electric propulsion system with take-off weight up to 300 kg. The works were carried out in order to learn about the possibility of design the unmanned air vehicle. Only components currently available on the aviation and automotive markets were used in the design.
Authors focus mainly on prototype propeller design that was manufactured in several copies for bench tests. The propeller has been designed to meet the construction and operational assumptions presented in the above study. The paper discusses design process, aerodynamic analysis and carbon composite manufacturing technology process. Furthermore, testing process of propellers on the measuring stand for testing propellers/rotors in hover is described. The tests were carried out for the angle of attack of the propeller blades obtained during aerodynamic analyzes . As can be seen, the values obtained in the experiment are different (higher) by approximately 7% than those resulting from aerodynamic analyzes. The mechanical power density is about 7- 8 kg/kW for the propellers

rotational speed of 1400 -1700 RPM. At lower speeds (1200-1300 RPM) power density is about 10 kg/kW. Thus, the design goal presented in Chapter 3 has been achieved.
Next tests are being prepared:

- For various angles of attack of propeller blades;
- for two propeller configurations (push and tractor propeller).

These tests, among other, will be used for further work on the prepared tool in the form of a model of the dynamics of multi-rotor and hybrid systems.

REFERENCES

[1] Certification Specifications and Acceptable Means of Compliance for Propellers (CS-P), 01 July 2020

[2] Ezertas, A., Yucekayali, A., Ortakaya, Y., *Hover performance assessment of 3 meter radius rotor on whirl tower*, 39th European Rotorcraft Forum, Moscow 2013

[3] Finger F.D., Braun C., and Bil C., *A Review of configuration design for distributed propulsion transitioning VTOL Aircraft*, Asia-Pacific International Symposium on Aerospace Technology, Seoul Korea, pp.1782-1796, 2017

[4] Klimczyk W.A., *Aerodynamic design and optimization of propellers for multirotor,* Aircraft Engineering and Aerospace Technology, Vol. 91, No. 1, pp. 21-30, 2022

[5] Kozaczuk K., *Composite technology development based on helicopter rotor blades,* Aircraft Engineering and Aerospace Technology, Vol. 92, No. 3, pp. 273-284, 2018

[6] Sobieszek, A., Wojtas, M., Composite rotor blades tests essential before mounting on gyroplane, Journal of KONES Powertrain and Transport, Vol. 23, No. 4, pp. 487-494, 2016

[7] Stanisławski J., *Simulation investigation of operational conditions of rotor for high-speed compound helicopter*, Journal of KONES Powertrain and Transport, Vol. 25, No. 1, pp. 263 – 370, 2018

[8] Stanisławski J., *Pattern of helicopter rotor loads and blade deformations in some states of flight envelope*, Transactions on aerospace research No. 1 Vol. 238, pp. 70-90, 2015

[9] Wilk J., *Validation of numerical models used for designing the composite blade for ILX-27 rotorcraft*, Transactions on aerospace research, No. 257, pp. 23-31, 2019

[10] Wojtas M., Czajkowski Ł., Szumański K, *Ground test stands for testing rotors in insulated conditions*, Transactions on aerospace research, Vol. 262, No.1, pp15-23, 2021

[11] Wojtas M., Czajkowski Ł., *Prototype test stand for testing insolated rotor systems*, Journal of KONES Powertrain and Transport, Vol. 26, No.3, pp257-264, 2019

[12] Wojtas M., Czajkowski Ł., Stanisławski J. and Szumański K., *Numerical analyses of different state of flight of new concept coaxial rotor dedicated to unmanned helicopters*, 45th European Rotorcraft Forum, Warsaw Poland, Vol. 1, pp.1472 -1479

[13] Zhao, Han, Dai and Hua, *Study on the Electromagnetic Design and Analysis of Axial Flux Permanent Magnet Synchronous Motors for Electric Vehicles,* Energies, Vol. 12, No. 18, 2019

[14] http://contrails.free.fr/

[15] http://sternaaircraft.com/

[16] https://www.sensenich.com/